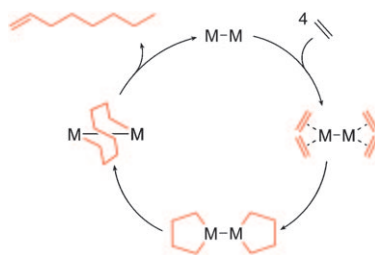


**2+2+2=6 and 2×4=8?** This concept explains the differences of selectivity between ethylene tri- and tetramerization by the capability of the ligands to form binuclear complexes that subsequently build up two metallacyclopentanes in one moiety. These two C4 units are then coupled to form 1-octene selectively (see scheme).



### Reaction Mechanisms

*S. Peitz, B. R. Aluri, N. Peulecke, B. H. Müller, A. Wöhl, W. Müller,\* M. H. Al-Hazmi, F. M. Mosa, U. Rosenthal\** ..... 7670–7676

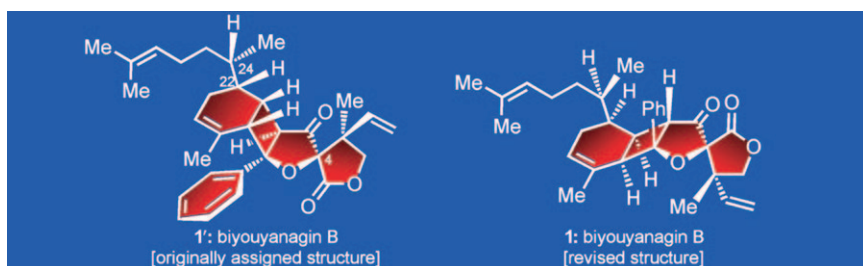
**An Alternative Mechanistic Concept for Homogeneous Selective Ethylene Oligomerization of Chromium-Based Catalysts: Binuclear Metallacycles as a Reason for 1-Octene Selectivity?**

## COMMUNICATIONS

### Natural Products

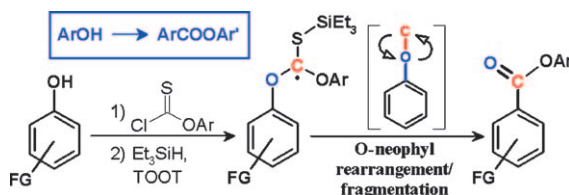
*K. C. Nicolaou,\* S. Sanchini, T. R. Wu, D. Sarlah* ..... 7678–7682

**Total Synthesis and Structural Revision of Biyouyanagin B**



**An intriguing chase** of the newly reported biyouyanagin B leads to its

total synthesis and structural revision from **1'** to **1**.



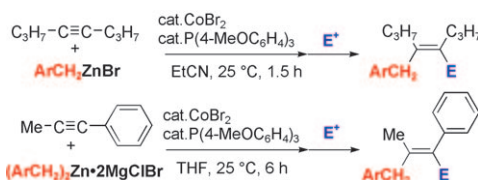
**Radical merry-go-round!** Diaryl thio-carbonates, available in a single step from phenols, can be directly transformed into benzoates by a new radical cascade that transposes O and C atoms at the aromatic core. The cascade bypasses the common Barton–

McCombie fragmentation in favor of the usually unfavorable O-neophyl rearrangement, which is rendered irreversible and efficient by a highly exothermic C–S bond scission in the O-centered radical (see scheme; FG=functional group).

### Cascade Reactions

*A. Baroudi, J. Alicea, I. V. Alabugin\** ..... 7683–7687

**Radical 1,2-O→C Transposition for Conversion of Phenols into Benzoates by O-Neophyl Rearrangement/Fragmentation Cascade**



**Carbometalation:** Cobalt salts catalyze benzylzincation of alkynes to afford benzylated multisubstituted alkenes with high regio- and stereoselectivity. The scope of the reaction is wide enough to apply unfunctionalized

alkynes as well as arylacetylenes. The reaction offers a new route to the regio- and stereoselective synthesis of an estrogen receptor antagonist (see scheme).

### Benzylation

*K. Murakami, H. Yorimitsu,\* K. Oshima\** ..... 7688–7691

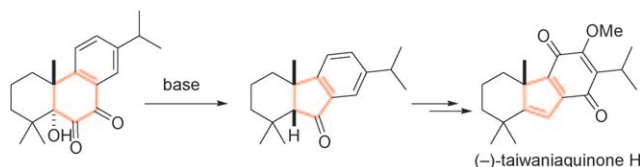
**Cobalt-Catalyzed Benzylzincation of Alkynes**



## Natural Products

C. K. Jana, R. Scopelliti,  
K. Gademann\* ..... 7692–7695

### A Synthetic Entry into the Taiwan-quinoids Based on a Biogenetic Hypothesis: Total Synthesis of (–)-Taiwaniaquinone H



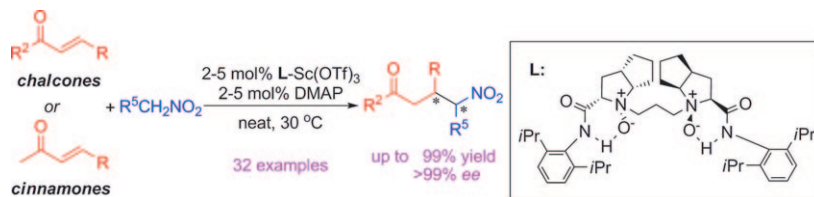
**Less carbon:** Following a biogenetic proposal, the unusual 6-5-6 carbon skeleton of C<sub>19</sub> taiwaniaquinoids was obtained by an intramolecular benzilic acid rearrangement from a C<sub>20</sub> precursor.

A protecting-group-free total synthesis then allowed for the preparation of (–)-taiwaniaquinone H (see scheme).

## Michael Addition

L. Wang, Q. Zhang, X. Zhou, X. Liu,  
L. Lin, B. Qin,\* X. Feng\* .. 7696–7699

### Asymmetric Conjugate Addition of Nitromethane to Enones Catalyzed by Chiral *N,N'*-Dioxide–Scandium(III) Complexes



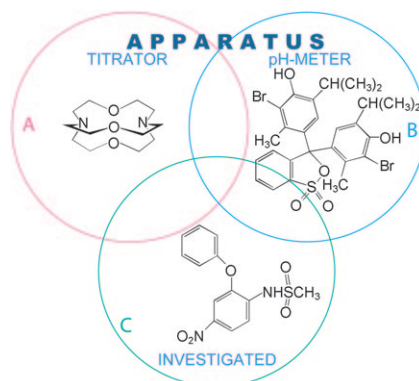
**Chalk it up as a “Sc”andal:** The asymmetric conjugate addition of chalcone and “cinnamone” derivatives to nitromethane has been realized by using a simple and efficient scandium(III)–*N,N'*-dioxide complex as the catalyst

(see scheme). In the presence of 2–5 mol % catalyst loading, the corresponding products were formed in excellent yields (up to 99 %) and enantioselectivities (up to > 99 % *ee*).

## Molecular Devices

G. Alibrandi,\* C. Lo Vecchio,  
A. Villari, I. Villari ..... 7700–7703

### Molecular Apparatus for Automatic Titrations

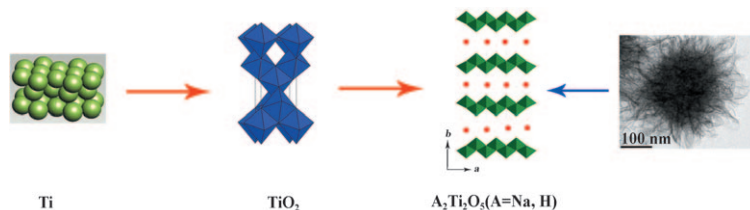


**Equipment free!** A composite kinetic molecular device formed by a molecular titrator ([1.1.1]cryptand (A)) and a molecular pH meter (bromothymol blue (B)) was used as a substitute for the usual physical apparatus to perform an automatic spectrophotometric determination of the p*K*<sub>a</sub> of nimesulide (C). The confinement of the whole apparatus inside the spectrophotometric cuvette makes high-throughput p*K*<sub>a</sub> and stability determination in pharmaceutical analysis possible.

## Electrochemistry

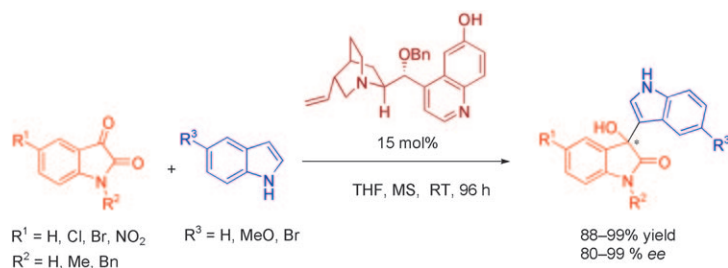
Y. Tang, Y. Lai, D. Gong, K.-H. Goh,  
T.-T. Lim, Z. Dong,\*  
Z. Chen\* ..... 7704–7708

### Ultrafast Synthesis of Layered Titanate Microspherulite Particles by Electrochemical Spark Discharge Spallation



**Bright sparks!** Hierarchical layered titanate microspherulite particles with large specific surface areas (406 m<sup>2</sup> g<sup>–1</sup>) and excellent adsorption abilities were quickly synthesized by a facile method

that simultaneously employed electrochemical anodization and spark discharge of the anodized oxide into a reactive solution (see figure).



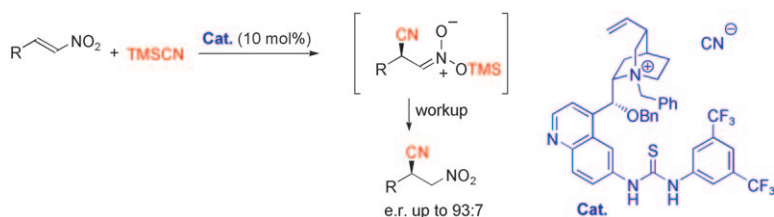
**Simple and selective:** An efficient organocatalytic enantioselective method for the synthesis of substituted-3-hydroxyoxindole derivatives with a quaternary chiral carbon has been developed. The cinchona alkaloid derived catalyst catalyses the Friedel–

Crafts-type addition of indole derivatives to the isatin derivatives under mild conditions to provide substituted 3-hydroxyoxindoles in good to excellent yields with high enantioselectivity (see scheme).

## Organocatalysis

P. Chauhan,  
 S. S. Chimni\* ..... 7709–7713

### Asymmetric Addition of Indoles to Isatins Catalysed by Bifunctional Modified Cinchona Alkaloid Catalysts



**New catalyst, new reaction:** The unprecedented cyano-silylation of nitroalkenes can be efficiently catalyzed by a bifunctional quinone derivative with tetraalkylammonium cyanide and thiourea moieties. The activation of the

nitroalkene by hydrogen bonding to the thiourea, together with the presence of an “active” cyanide, provides a new mode of activation that leads to products in high yields and good selectivities (see scheme).

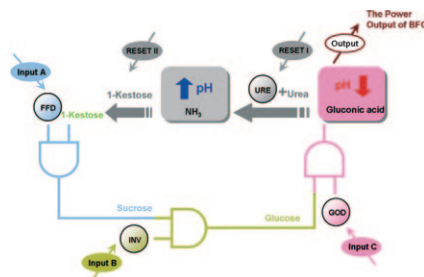
## Asymmetric Organocatalysis

P. Bernal, R. Fernández,\*  
 J. M. Lassaletta\* ..... 7714–7718

### Organocatalytic Asymmetric Cyano-silylation of Nitroalkenes



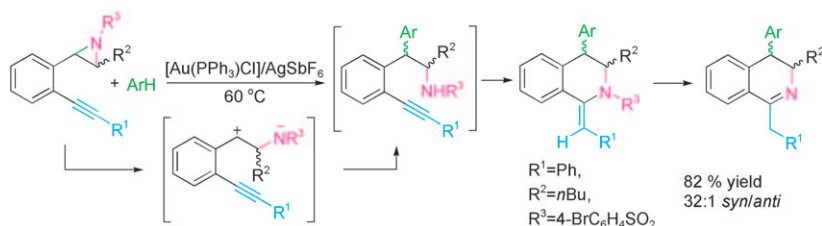
**Locked up!** A novel self-powered, reusable biofuel cell (BFC) based bio-computing security system mimicking a keypad lock device using enzyme-based concatenated AND logic gates has been developed (see figure; FFD = fructan beta-fructosidase, INV = invertase, GOD = glucose oxidase, URE = urease).



## Molecular Devices

M. Zhou, X. Zheng, J. Wang,\*  
 S. Dong\* ..... 7719–7724

### A Self-Powered and Reusable Biocomputing Security Keypad Lock System Based on Biofuel Cells



**Aziridinyll alkynes strike gold:** A novel gold(I)-catalyzed domino transformation of aziridinyll alkynes with arenes to construct 1,2,3,4-tetrahydroisoquinoline and 3,4-dihydroisoquinoline structural motifs (see scheme), especially sterically congested *syn*-3,4-disubsti-

tuted 1,2,3,4-tetrahydroisoquinolines, is described. A plausible mechanism proceeding through a benzylic cation is given based upon deuterium-labeling and control experiments as well as the observed diastereoselectivities.

## Gold-Catalyzed Synthesis

Z. Zhang, M. Shi\* ..... 7725–7729


### Gold(I)-Catalyzed Domino Reaction of Aziridinyll Alkynes

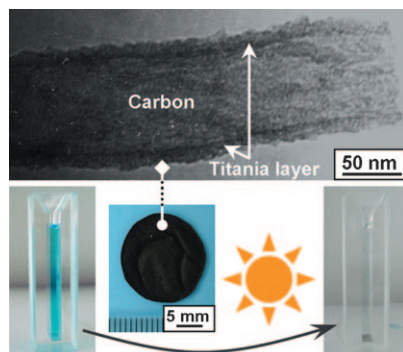


## FULL PAPERS

### Biomimetic Materials

X. Liu, Y. Gu, J. Huang\* ... 7730–7740


 **Hierarchical, Titania-Coated, Carbon Nanofibrous Material Derived from a Natural Cellulosic Substance**

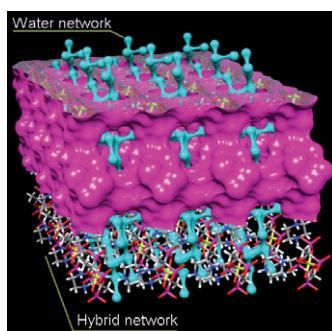


**Gift from nature:** A hierarchical titania–carbon hybrid material composed of porous carbon nanofibers coated with a uniform anatase titania film (see figure) was fabricated by using a natural cellulosic substance (filter paper) as both a scaffold and carbon precursor. The material possesses enhanced photocatalytic degradation efficiency with respect to different dyes and improved photoreduction performance of silver cations to silver nanoparticles.

### Water Chemistry

J. Rocha,\* F.-N. Shi, F. A. A. Paz, L. Mafra, M. Sardo, L. Cunha-Silva, J. Chisholm, P. Ribeiro-Claro, T. Trindade ... 7741–7749


 **3D–2D–0D Stepwise Deconstruction of a Water Framework Templated by a Nanoporous Organic–Inorganic Hybrid Host**

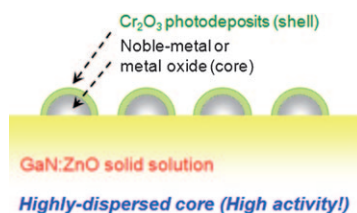


**Ice framework deconstruction:** The supramolecular salt  $[H_2pip]_3[Ge(hedp)_2] \cdot 14 H_2O$  ( $pip = C_4H_{12}N_2^{2+}$ ;  $hedp = C_2H_3P_2O_7^{5-}$ ) features 3D interpenetrated networks of hydrogen-bonded water molecules and a hybrid matrix (see figure). The ‘ice’ framework is stable up to around 22 °C, and its deconstruction occurs in a stepwise fashion from 3D to 2D and discrete water aggregates (0D). In the process, however, the long-range order of the hybrid host is preserved.

### Water Splitting

K. Maeda, N. Sakamoto, T. Ikeda, H. Ohtsuka, A. Xiong, D. Lu, M. Kanehara, T. Teranishi, K. Domen\* ... 7750–7759


 **Preparation of Core–Shell-Structured Nanoparticles (with a Noble-Metal or Metal Oxide Core and a Chromia Shell) and Their Application in Water Splitting by Means of Visible Light**

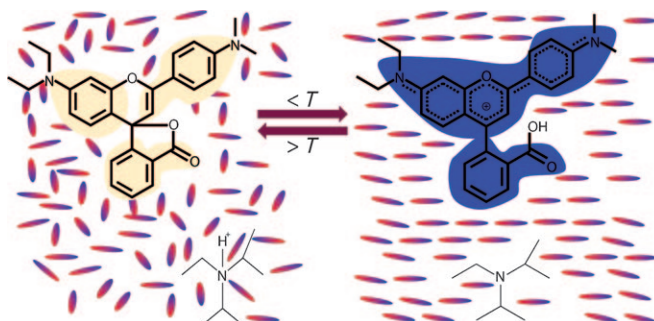


**Breaking up is hard to do:** Photodeposition of chromia onto nanoparticulate co-catalysts (metals or metal oxides) onto a GaN:ZnO solid solution to form a core–shell configuration resulted in enhanced activity for photocatalytic overall water splitting under visible light (see figure).

### Spiro Compounds

R. Gavara, C. A. T. Laia, A. J. Parola, F. Pina\* ... 7760–7766

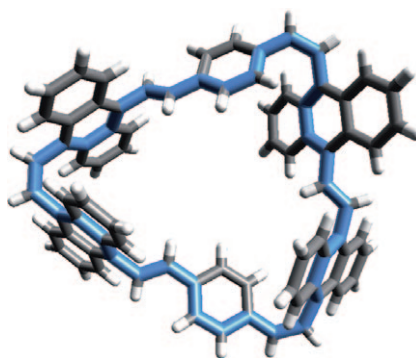
 **Formation of a leuco Spirolactone from 4-(2-Carboxyphenyl)-7-diethylamino-4'-dimethylamino-1-benzopyrylium: Design of a Phase-Change Thermochromic System Based on a Flavylium Dye**



**A new phase-change** thermochromic system is described (see scheme), which is based on the 4-(2-carboxy-

phenyl)-7-diethylamino-4'-dimethylamino-1-benzopyrylium dye and its leuco form, a spirolactone.

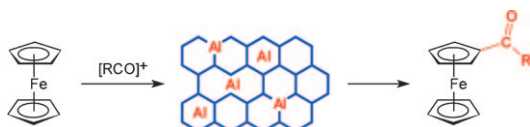
**Do the twist!** Möbius and Hückel conformations (single- and double-twisted) were crystallized from a solution of a cyclophane with a [36]annulene periphery in different solvents (see figure). All new structures were clearly identified by X-ray analysis and confirmed by DFT calculations. An energetically favorable triple-twisted conformation of the annulene was also located by using DFT calculations.



## Annulenes

A. R. Mohebbi, E.-K. Mucke,  
G. R. Schaller, F. Köhler,  
F. D. Sönnichsen, L. Ernst, C. Näther,  
R. Herges\* ..... 7767–7772

## Singly and Doubly Twisted [36]Annulenes: Synthesis and Calculations



**A hole-istic solution:** AIKIT-5 mesoporous molecular sieves, which are readily prepared by direct template synthesis with varying Al/Si ratios, proved to

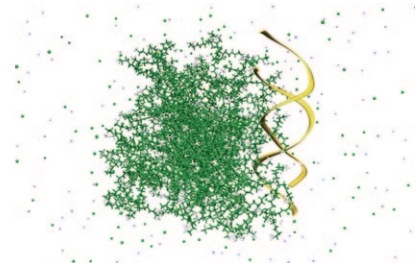
be efficient, selective, and recyclable catalysts for selective monoacylation of ferrocene with bulky acylation agents (see image).

## Acylation

D. Procházková, M. Bejblová, J. Vlk,  
A. Vinu, P. Štěpnička,  
J. Čejka\* ..... 7773–7780

## Selective Monoacylation of Ferrocene with Bulky Acylating Agents over Mesoporous Sieve AIKIT-5

**Snapshots taken from molecular dynamics simulations** of PAMAM generations G6 in a complex with GL3 siRNA at pH 7.4 are shown here. Dendrimers are depicted as colored sticks, the terminal  $\text{NH}_3^+$  groups as white balls and sticks. The siRNA is outlined as a golden ribbon. Sodium and chlorine counterions are portrayed as purple and green spheres, respectively. Water is omitted for clarity.



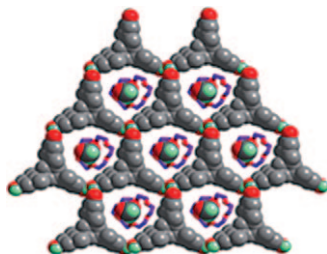
## siRNA/PAMAM Interactions

G. M. Pavan, P. Posocco,\*  
A. Tagliabue, M. Maly, A. Malek,  
A. Danani, E. Ragg, C. V. Catapano,  
S. Priol ..... 7781–7795

## PAMAM Dendrimers for siRNA Delivery: Computational and Experimental Insights



**A sterically-engineered** rigid trigonal triphenol undergoes O–H...O hydrogen-bonded self-assembly in the presence of [18]crown-6 and neutral (MeOH/water, MeOH/MeNO<sub>2</sub>) or ionic guest species (KI/KAcAc) to furnish novel multicomponent assemblies, that is, guest⊂guest⊂host, which typify Russian dolls.



## Self-Assembly

J. N. Moorthy,\*  
P. Natarajan ..... 7796–7802

## Guest⊂Guest⊂Host Multicomponent Molecular Crystals: Entrapment of Guest⊂Guest in Honeycomb Networks Formed by Self-Assembly of 1,3,5-Tri(4-hydroxyaryl)benzenes



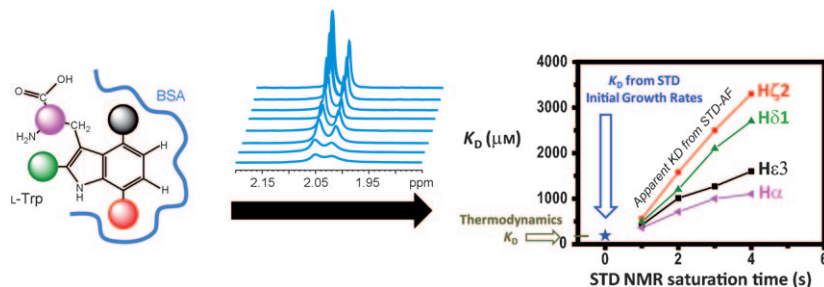
## Receptor–Ligand Interactions

J. Angulo,\* P. M. Enríquez-Navas,  
P. M. Nieto\* ..... 7803–7812



VIP

### Ligand–Receptor Binding Affinities from Saturation Transfer Difference (STD) NMR Spectroscopy: The Binding Isotherm of STD Initial Growth Rates



The initial growth rates of the STD amplification factors cancel out spurious experimental factors due to protein–ligand rebinding, which affects the accumulation of saturation in the free ligand and allows accurate deter-

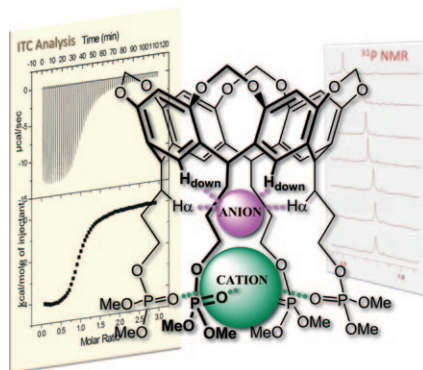
minations of dissociation constants ( $K_D$ ) from the variation of STD NMR spectroscopy values with the receptor–ligand ratio (BSA = bovine serum albumin, see figure).

## Cavitand Receptors

F. Tancini, T. Gottschalk,  
W. B. Schweizer, F. Diederich,\*  
E. Dalcanele\* ..... 7813–7819



### Ion-Pair Complexation with a Cavitand Receptor



**Phosphotriester cavitand:** The lower rim pocket of a methylene-bridged cavitand, preorganized for anion binding, has been decorated with four phosphotriester residues at the termini of the feet for counterion complexation by hydrogen bonding (see figure). The combination of the two modes of interaction leads to the efficient binding of primary ammonium salts in the form of ion pairs.

## Electron Transfer

M. Murakami, K. Ohkubo,  
S. Fukuzumi\* ..... 7820–7832



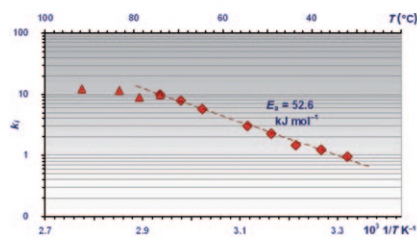
### Inter- and Intramolecular Photo-induced Electron Transfer of Flavin Derivatives with Extremely Small Reorganization Energies



**Long-lived charge separation:** 10-[4'-(*N,N*-Dimethylamino)phenyl]-isoalloxazine (DMA-FI) undergoes efficient intramolecular photoinduced electron transfer to afford the charge-separated

(CS) state that has the longest CS lifetime (2.1 ms) by preventing the intermolecular back electron transfer in solution at 298 K (see figure).

**Finding the parameters:** An extensive experimental parameter study has been carried out on a novel ethylene trimerization catalyst system. Ethylene and catalyst concentration were found to affect the initial activity, and the activation energy ( $E_a$ ) was determined by studying temperature dependencies (see figure).

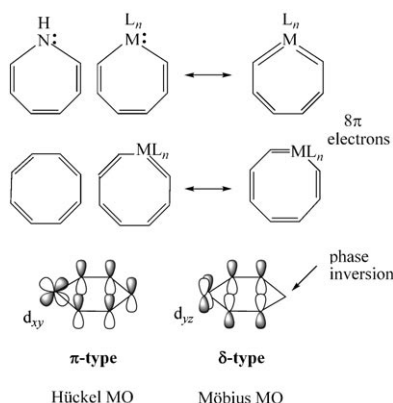


## Homogeneous Catalysis

A. Wöhl, W. Müller,\* S. Peitz,  
N. Peulecke, B. R. Aluri, B. H. Müller,  
D. Heller, U. Rosenthal,\*  
M. H. Al-Hazmi,  
F. M. Mosa ..... 7833–7842

**Influence of Process Parameters on the Reaction Kinetics of the Chromium-Catalyzed Trimerization of Ethylene**

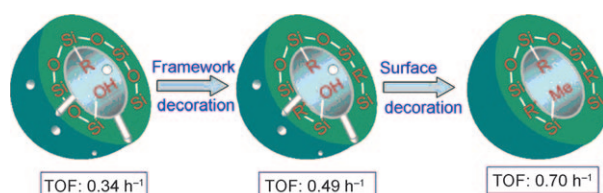
**Without a twist:** Several seven- and eight-membered metallacycles that contain transition-metal atoms with available d orbitals of appropriate symmetry and orientation are computationally demonstrated to be “Möbius” aromatic with eight electrons involved in the cyclic delocalization (see figure).



## Aromaticity

M. Mauksch,\*  
S. B. Tsogoeva\* ..... 7843–7851

**Demonstration of “Möbius” Aromaticity in Planar Metallacycles**



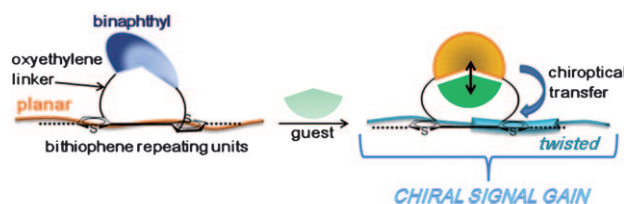
**Hollowed be thy name:** L-Prolinamide-functionalized hollow nanospheres with different surface hydrophobicity/hydrophilicity were prepared. The catalytic activity of the hollow nano-

spheres was clearly improved after framework and surface hydrophobic decoration (see graphic; TOF = turnover frequency) for an asymmetric aldol reaction in the presence of water.

## Nanostructures

J. Gao, J. Liu, J. Tang, D. Jiang, B. Li,  
Q. Yang\* ..... 7852–7858

**Chirally Functionalized Hollow Nanospheres Containing L-Prolinamide: Synthesis and Asymmetric Catalysis**



**In a twist:** Upon inclusion of a chiral cationic guest in the cavity of a newly synthesized chiral crown ether–polythiophene conjugate, the bithiophene unit was twisted to shorten the effective conjugation length of the polythio-

phene backbone, enabling us to sense the guest binding by reading out the amplified optical signal gains arising from the backbone structure change (see figure).

## Chirality-Sensing Polymer

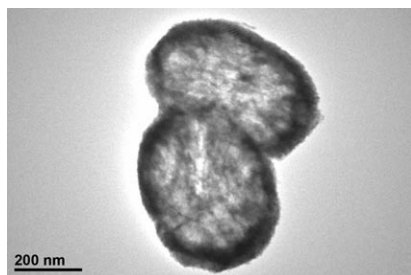
G. Fukuhara,\* Y. Inoue\* ... 7859–7864

**Chirality-Sensing Binaphthocrown Ether–Polythiophene Conjugate**

## Photocatalysis

A. K. Sinha, M. Basu, M. Pradhan,  
S. Sarkar, T. Pal\* ..... 7865–7874

### Fabrication of Large-Scale Hierarchical ZnO Hollow Spheroids for Hydrophobicity and Photocatalysis

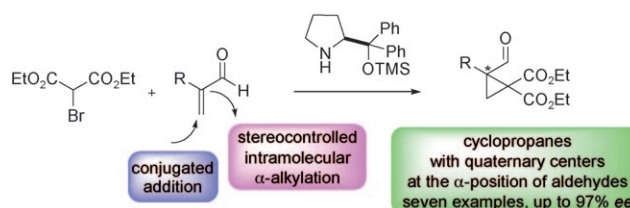


**Cocoonlike structures:** A simple procedure allows the preparation of a hollow spheroid ZnO material like a natural cocoon (see figure). A bubble-template strategy is designed through a modified hydrothermolysis (MHT) reaction to construct hollow ZnO nanostructures. The hollow spheroids allow multiple reflections of UV-visible light within the interior cavity that facilitates efficient usage of the light source. The 3D nanococoon architecture improves the superhydrophobicity and photocatalytic performances of these materials.

## Organocatalysis

V. Terrasson, A. van der Lee,  
R. Marcia de Figueiredo,\*  
J. M. Campagne\* ..... 7875–7880

### Organocatalyzed Cyclopropanation of $\alpha$ -Substituted $\alpha,\beta$ -Unsaturated Aldehydes: Enantioselective Synthesis of Cyclopropanes Bearing a Chiral Quaternary Center



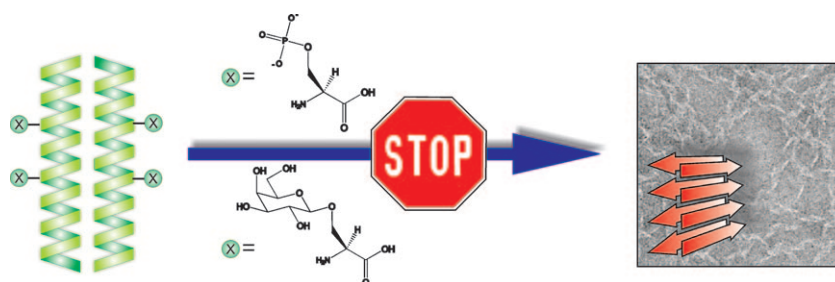
**Enantioselective cyclopropanation** of  $\alpha$ -substituted  $\alpha,\beta$ -unsaturated aldehydes is reported (see scheme). The transformation is driven by diphenyl-

prolinol trimethylsilyl ether. A variety of cyclopropanes bearing a chiral quaternary stereocenter at the  $\alpha$ -position of the aldehydes is obtained.

## Amyloid Formation

M. Broncel, J. A. Falenski,  
S. C. Wagner, C. P. R. Hackenberger,  
B. Kokscha\* ..... 7881–7888

### How Post-Translational Modifications Influence Amyloid Formation: A Systematic Study of Phosphorylation and Glycosylation in Model Peptides



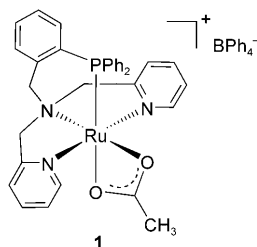
**All against amyloid formation:** An important step towards the understanding of the impact of phosphorylation and glycosylation on amyloid formation has been made (see figure). It

has been demonstrated that even single phosphorylation is sufficient to completely inhibit fibrilization, whereas glycosylation showed more diverse effects.

## Homogeneous Catalysis

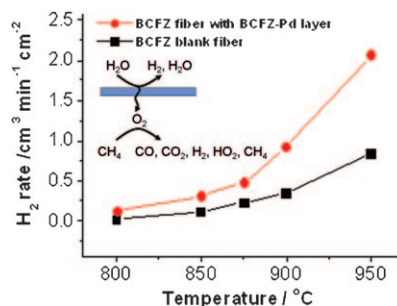
P. N. Liu, F. H. Su, T. B. Wen,  
H. H.-Y. Sung, I. D. Williams,  
G. Jia\* ..... 7889–7897

### Selective and Efficient Cycloisomerization of Alkynols Catalyzed by a New Ruthenium Complex with a Tetradentate Nitrogen–Phosphorus Mixed Ligand



**Go complex!** The new air-stable ruthenium complex **1** is an effective catalyst for the *endo* cycloisomerization of a range of alkynols to give exclusively *endo*-cyclic enol ethers of five-, six-, and seven-membered rings in high yields under nonbasic conditions (see scheme). The catalytic reactions can be carried out with a low loading of catalyst without additional co-catalyst.

**Go with the flow:** Perovskite  $\text{BaCo}_x\text{Fe}_y\text{Zr}_{1-x-y}\text{O}_{3-\delta}$  (BCFZ) oxygen permeable membranes were used as reactors to shift the equilibrium of water dissociation for hydrogen production. The hydrogen production rate was increased from 0.7 to  $2.1 \text{ mL min}^{-1} \text{ cm}^{-2}$  at  $950^\circ\text{C}$  after depositing a BCFZ-Pd porous layer onto the BCFZ hollow-fiber membrane (see figure).



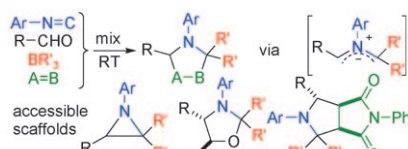
## Membranes

H. Jiang,\* F. Liang, O. Czuprat, K. Efimov, A. Feldhoff, S. Schirmer, T. Schiestel, H. Wang, J. Caro\* ..... 7898–7903

**Hydrogen Production by Water Dissociation in Surface-Modified  $\text{BaCo}_x\text{Fe}_y\text{Zr}_{1-x-y}\text{O}_{3-\delta}$  Hollow-Fiber Membrane Reactor with Improved Oxygen Permeation**



**One step, four components:** An early report from the 1960s has been reformulated into a novel family of multicomponent reactions that leads to aziridine, oxazolidine and pyrrolidine scaffolds just by mixing the reactants (see picture). The scope and mechanistic course of these domino processes are determined. Solid-phase protocols allow straightforward preparations and even permit chemo-differentiation of pseudo-equivalent inputs.



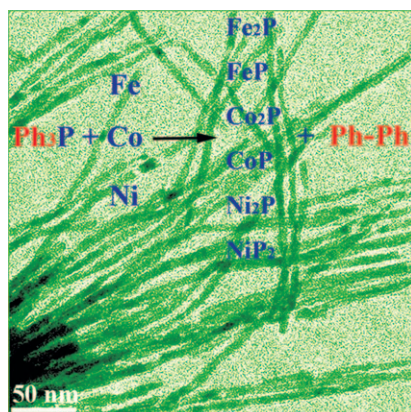
## Multicomponent Reactions

N. Kielland, F. Catti, D. Bello, N. Isambert, I. Soteras, F. J. Luque, R. Lavilla\* ..... 7904–7915

**Boron-Based Dipolar Multicomponent Reactions: Simple Generation of Substituted Aziridines, Oxazolidines and Pyrrolidines**



**Transition metals react with  $\text{PPh}_3$**  in vacuum-sealed tubes at  $350\text{--}400^\circ\text{C}$  to form metal phosphide nanowires by Ullmann-type reactions involving phenyl radicals (see general equation, superimposed on a TEM image of  $\text{Co}_2\text{P}$  nanowires). The phase (stoichiometry) of the phosphide nanostructures can be controlled by means of the metal/ $\text{PPh}_3$  molar ratio and concentration, reaction temperature and time, and they exhibit interesting phase- and composition-dependent magnetic properties.



## Phosphide Nanowires

J. Wang, Q. Yang,\* Z. Zhang, S. Sun ..... 7916–7924

**Phase-Controlled Synthesis of Transition-Metal Phosphide Nanowires by Ullmann-Type Reactions**



\* Author to whom correspondence should be addressed



Supporting information on the WWW (see article for access details).



Full Papers labeled with this symbol have been judged by two referees as being “very important papers”.



A video clip is available as Supporting Information on the WWW (see article for access details).

## SERVICE

Spotlights ..... 7664    Author Index ..... 7928    Keyword Index ..... 7929    Preview ..... 7931

Issue 25/2010 was published online on June 25, 2010